Influence of damping on proton energy loss in plasmas of all degeneracies

Manuel D. Barriga-Carrasco
E.T.S.I. Industriales, Universidad de Castilla-La Mancha, E-13071 Ciudad Real, Spain
(Received 9 May 2006; revised manuscript received 12 March 2007; published 20 July 2007)

The purpose of the present paper is to describe the effects of electron-electron collisions on the stopping power of plasmas of any degeneracy. Plasma targets are considered fully ionized so electronic stopping is only due to the free electrons. We focus our analysis on plasmas which electronic density is around solid values $n_e \simeq 10^{23}$ cm^{-3} and which temperature is around $T \simeq 10$ eV; these plasmas are in the limit of weakly coupled plasmas. This type of plasma has not been studied extensively though it is very important for inertial confinement fusion. The electronic stopping is obtained from an exact quantum mechanical evaluation, which takes into account the degeneracy of the target plasma, and later it is compared with common classical and degenerate approximations. Differences are around 30% in some cases which can produce bigger mistakes in further energy deposition and projectile range studies. Then we consider electron-electron collisions in the exact quantum mechanical electronic stopping calculation. Now the maximum stopping occurs at velocities smaller than for the calculations without considering collisions for all kinds of plasmas analyzed. The energy loss enhances for velocities smaller than the velocity at maximum while decreases for higher velocities. Latter effects are magnified with increasing collision frequency. Differences with the same results for the case of not taking into account collisions are around 20% in the analyzed cases.

DOI: 10.1103/PhysRevE.76.016405 PACS number(s): 52.40.Mj, 52.65.Yy, 52.20.Fs, 52.25.Mq

I. INTRODUCTION

The energy loss of charged particles in a free electron gas is of considerable interest to actual slowing-down problems. This is a topic of relevance to understand the beam-target interaction in the contexts of particle driven fusion [1,2]. The energy losses of ions moving in an electron gas can be studied through the stopping power of the medium. Dielectric formalism has become one of the most used methods to describe this stopping power. The use of this formalism was introduced by Fermi [3]. Subsequent developments made it possible to extend the dielectric formalism to provide a more comprehensive description of the stopping of ions in matter [4,5]. For dilute plasmas, the dielectric formulation of the energy-loss rate was first studied by Pines and Bohm [6], Akhiezer and Sitenko [7], and other scientists. A large number of calculations of electronic stopping forces of ions and electrons in plasmas have been carried out since then using the classical linear response function in the random phase approximation (RPA) (see [8] for a complete list). This approximation consists of considering the effect of the particle as a perturbation, so that the energy loss is proportional to the square of the particle charge. Then the theory of slowing-down is simplified to a treatment of the properties of the medium only, and a linear description of these properties may be applied. The linear properties of an infinite gas of free electrons can be described by its dielectric function.

The RPA is usually valid for high-velocity projectiles and in the weak coupling limit of an electron gas, i.e., $\Gamma \ll 1$. The coupling parameter, $\Gamma = \frac{E_F}{\pi k_F (E_F + k_B T)}$ [9], measures the ratio between potential and kinetic energies of the electrons at any degeneracy of the plasma, where E_F and k_F are Fermi energy and Fermi wave number, respectively, and T is the plasma temperature. In this work we will study plasmas with $\Gamma \lesssim 1$ so RPA is not sufficient and the collisions between the electrons of the target gas have to be taken into account. RPA predicts an infinite lifetime for target plasma plasmons, whereas it is well-known that in real materials these excitations are damped. It seems to be a straightforward substitution, the replacement of $\epsilon(k,\omega)$ by $\epsilon(k,\omega+i\nu)$, where ν represents the electron-electron collision frequency, but it is erroneous, as it does not conserve the local particle number. Mermin [10] and later Das [11] derived an expression for the dielectric function taking account of the finite lifetime of the plasmons and also preserving the local particle density. Recently, an extended dielectric function has been considered which conserves also momentum and energy [12–14], but it is somewhat involved and it has only small differences with the Mermin dielectric function. In previous investigations for solids, we determined ν by fitting $-\mathrm{Im}[\epsilon^{-1}(0,\omega+i\nu)]$ to experimental optical energy loss functions [15–17], but this frequency must be calculated *a priori* for plasmas. Many works have been devoted to calculate this frequency [18–20], but here we treat it as a free parameter as in other investigations [21–23].

Theoretical studies of the dielectric function are usually focused on two main domains of plasma physics. (a) Dense plasmas at low temperatures, usually described with degenerate electron gas models and the use of quantum mechanical methods, as plasmas of interest for inertial confinement fusion (ICF). (b) Dilute plasmas at high temperatures, usually described with nondegenerate electron gas models and the use of a classical description; it includes the case of plasmas of interest for magnetic confinement fusion (MCF). The transition from nondegenerate to degenerate plasmas in the range of high densities ($n_e \simeq 10^{23}$–10^{27} e cm^{-3}) is a subject of much interest for current studies of ICF. The approach to those extreme conditions is being tested nowadays using ion beams generated by lasers [24–30].

The Mermin dielectric function has been successfully applied to solids (dense degenerate electron gas) [31–33] and for classical plasmas (nondegenerate electron gas) [34,35]. In

this paper we extend our calculations to consider the effects of electron-electron collisions in RPA for an electron gas of any degeneracy. In the past, Skupsky [36], Arista and Brandt [37], and Maynard and Deutsch [38] have considered the calculation of the energy loss in a quantum mechanical plasma of arbitrary degeneracy but without considering damping due to these collisions. The final purpose of this work is to include this theoretical model in our computer code, TAMIM (transport of atomic and molecular ions in matter), formerly MBC-ITFIP [39]. There is no doubt that a user-friendly computer code to calculate the energy loss of ions in plasmas of any degeneracy can be of great help to the scientific community.

This paper is divided into two main sections. In Sec. II the dielectric function of plasmas of any degeneracy which takes into account plasma electron-electron collisions is obtained. Then in Sec. III, we use the latter dielectric function to calculate proton electronic stopping for a different kind of plasma targets. The last section also evaluates the influence of the collisions on the electronic stopping.

II. DIELECTRIC FUNCTION

In this section, we are going to develop the dielectric function $\epsilon(k,\omega)$ in terms of the wave number k and of the frequency ω provided by a consistent quantum mechanical analysis. The dielectric response of the electronic medium is calculated in the random phase approximation (RPA). We use atomic units (a.u.), $e=\hbar=m_e=1$, to simplify formulas. The RPA analysis yields to the expression [4]

$$\epsilon(k,\omega) = 1 + \frac{1}{\pi^2 k^2}\int d^3k' \frac{f(\vec{k}+\vec{k}') - f(\vec{k}')}{\omega + i\nu - (E_{\vec{k}+\vec{k}'} - E_{\vec{k}'})}, \quad (1)$$

where $E_{\vec{k}}=k^2/2$. The temperature dependence is included through the Fermi-Dirac function

$$f(\vec{k}) = \frac{1}{1+\exp[\beta(E_k-\mu)]}, \quad (2)$$

where $\beta=1/k_BT$ and μ is the chemical potential of the plasma with electron density n_e and temperature T. In this part of the analysis we assume the absence of collisions so the damping constant approaches zero, $\nu\to 0^+$.

The degeneracy of the plasma depends on its temperature and is measured through the degeneracy parameter D which is the inverse of the reduced temperature θ,

$$D \equiv \frac{1}{\theta} \equiv \frac{E_F}{k_BT}. \quad (3)$$

Then obviously, degenerate plasmas are those for which $D \gg 1$ and for nondegenerate plasmas we have $D \ll 1$. The chemical potential μ depends on D through the expression

$$\frac{2}{3}D^{3/2} = F_{1/2}(\beta\mu) = \int_0^\infty \frac{x^{1/2}}{1+\exp(x-\beta\mu)}dx, \quad (4)$$

where $F_{1/2}$ is the Fermi integral of order 1/2.

The dielectric function can be separated into its real and imaginary parts

$$\epsilon(k,\omega) = \epsilon_r(k,\omega) + i\epsilon_i(k,\omega). \quad (5)$$

$\epsilon_r(k,\omega)$ can be directly obtained from Eq. (1) [40],

$$\epsilon_r(k,\omega) = 1 + \frac{1}{4z^3\pi k_F}[g(u+z) - g(u-z)], \quad (6)$$

where $g(x)$ corresponds to

$$g(x) = \int_0^\infty \frac{ydy}{\exp(Dy^2-\beta\mu)+1} \ln\left|\frac{x+y}{x-y}\right|, \quad (7)$$

and $u=\omega/kv_F$ and $z=k/2k_F$ are the common dimensionless variables [4]. $v_F=k_F=\sqrt{2E_F}$ is Fermi velocity in a.u.

In the limit of high degeneracy, $D\gg 1$,

$$g(x) \simeq x + \frac{1}{2}(1-x^2)\ln\left|\frac{1+x}{1-x}\right|, \quad (8)$$

which substituted in Eq. (6) gives the Lindhard dielectric function for a degenerate plasma [4]. In the opposite limit, high temperatures, $D\ll 1$,

$$g(x) \simeq \frac{2}{3}D^{1/2}\Theta(D^{1/2}x), \quad (9)$$

where $\Theta(x)$ is the plasma dispersion function [41]

$$\Theta(x) = \frac{1}{\sqrt{\pi}}\int_{-\infty}^{\infty}\frac{\exp(-p^2)}{x-p}dp, \quad (10)$$

recovering the results for classical plasmas [35,42].

The function $\epsilon_i(k,\omega)$ also follows from Eq. (1) [40],

$$\epsilon_i(k,\omega) = \frac{1}{8z^3k_F}\theta\ln\left[\frac{1+\exp[\beta\mu - D(u-z)^2]}{1+\exp[\beta\mu - D(u+z)^2]}\right]. \quad (11)$$

Although this is an exact result for all plasma degeneracies, it has very interesting limiting values for the plasmas of cases (a) and (b). For high degenerate plasmas $D\gg 1$, $\beta\mu \simeq D$ then

$$\epsilon_i(k,\omega) \simeq \frac{1}{8z^3k_F}\theta\ln\left[\frac{1+\exp\{D[1-(u-z)^2]\}}{1+\exp\{D[1-(u+z)^2]\}}\right], \quad (12)$$

and for $D\to\infty$

$$\epsilon_i(k,\omega) \simeq \begin{cases} \dfrac{1}{8z^3k_F}\dfrac{\omega}{E_F}, & (u\pm z)^2 < 1, \\ \dfrac{1}{8z^3k_F}[1-(u-z)^2], & (u-z)^2 < 1 < (u+z)^2 \\ 0, & 1 < (u-z)^2 \end{cases}, \quad (13)$$

giving rise to the case of a degenerate plasma [4]. For nondegenerate plasmas $D\ll 1$, and $\hbar\to 0$ Eq. (11) transforms into

$$\epsilon_i(k,\omega) = \frac{\omega n_e}{k^3}(2\pi\beta)^{3/2}\exp\left(-\frac{\omega^2\beta}{2k^2}\right), \quad (14)$$

which is the classical result [35,42].

We will see in Sec. III that for ion stopping considerations, it is worth defining the energy loss function (ELF),

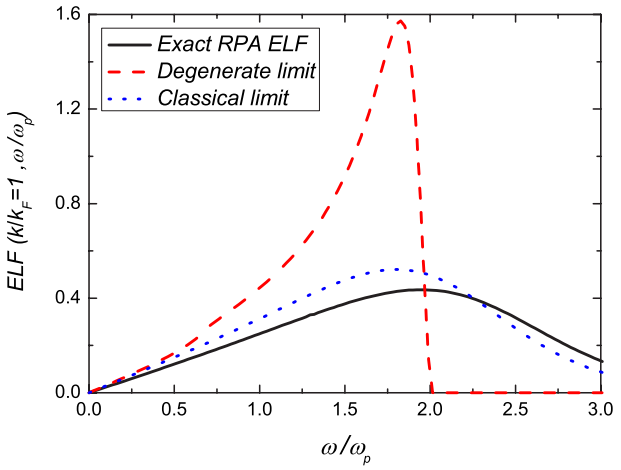

FIG. 1. (Color online) RPA energy loss function dependence with ω/ω_p when $k/k_F=1$, for a $T=10$ eV and $n_e=10^{23}$ cm^{-3} plasma ($D=0.785$). It is compared with degenerate and classical limits.

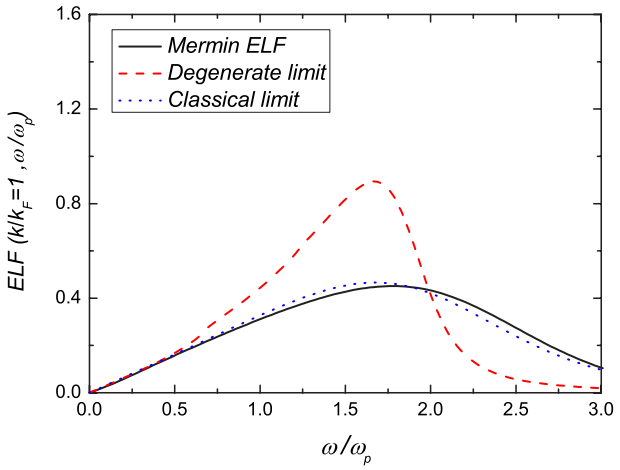

FIG. 2. (Color online) Mermin energy loss function dependence with ω/ω_p when $k/k_F=1$, for a $T=10$ eV and $n_e=10^{23}$ cm^{-3} plasma ($D=0.785$). It is compared with degenerate and classical limits. The collision frequency is $\nu=4$ fs^{-1}.

$$\mathrm{ELF} \equiv \mathrm{Im}\left(\frac{-1}{\epsilon(k,\omega)}\right). \tag{15}$$

Figure 1 shows the ELF's dependence with ω/ω_p when $k/k_F=1$, for a $T=10$ eV and $n_e=10^{23}$ cm^{-3} plasma. $\omega_p=\sqrt{4\pi n_e}$ is the plasma frequency. The exact calculation is achieved from Eqs. (7) and (11) which takes into account the degeneracy of the electron plasma, in this case the degeneracy parameter is $D=0.785$. The last curve is compared with the ELFs obtained for the limiting cases of high degeneracy $D\gg 1$ and high temperatures, $D\ll 1$. For high degeneracies we use the quantum mechanical approach of Eqs. (8) and (13) while for the high temperatures we employ the classical approach of Eqs. (9) and (14). As we can see the classical approximation is closer to the exact case which contemplates the degeneracy of the plasma. This can be a rough method to check if any approximation, quantum or classical, is well-suited for a specific case.

As mentioned in the Introduction, the random phase approximation (RPA) predicts an infinite life for plasmons, whereas it is well-known that in real materials these excitations are damped. Thus it is easy to think of substituting ω by $\omega+i\nu$ in the RPA dielectric function, obtaining the relaxation time approximation (RTA), where ν represents the electron-electron collision frequency. This method is erroneous as it does not conserve the local particle number or density. Mermin dielectric function [10] is derived using an expansion of the local equilibrium distribution function to conserve the local particle number

$$\epsilon_{\mathrm{M}}(k,\omega) = 1 + \frac{(\omega+i\nu)[\epsilon(k,\omega+i\nu)-1]}{\omega+i\nu[\epsilon(k,\omega+i\nu)-1]/[\epsilon(k,0)-1]}, \tag{16}$$

where $\epsilon(k,\omega+i\nu)$ is the RPA dielectric function from Eq. (5) in the RTA case. It is easy to see that when $\nu\to 0$, the Mermin function reproduces the RPA one. We checked in [35] that the Mermin method is the most appropriate for calculating the energy loss. In general, collision frequency ν is contributed from electron-electron and electron-ion collisions; but in this paper we take into account only the electron-electron collisions, in order to avoid considering a dependence of the stopping with the charge and mass of the target ions. Also ν will be considered as a free parameter to see the evolution of the dielectric function and the electronic stopping with the collision frequency. Its values will be chosen close to the ones according to the theory of Braginskii-Spitzer [43,44],

$$\nu = \nu(D) = \frac{16\sqrt{2}D^{3/2}\ln n_e^{1/2}/D^{3/2}}{9\pi\sqrt{\pi}}\ \text{(a.u.)}, \tag{17}$$

where $\ln n_e^{1/2}/D^{3/2}$ is the Coulomb logarithm. As we see, ν only depends on the degeneracy of the plasma.

Figure 2 shows the Mermin energy loss function dependence with ω/ω_p when $k/k_F=1$, for a $T=10$ eV and $n_e=10^{23}$ cm^{-3} plasma ($D=0.785$). In this case, we choose a value from Eq. (17), $\nu=4$ fs^{-1}. The solid line represents the Mermin ELF taking into account the degeneracy of plasma, the dashed line corresponds to the Mermin ELF using the high degeneracy limit of the dielectric function, and the dotted line is the Mermin ELF considering the classical approximation of the dielectric function. Compared with Fig. 1 the three new ELFs turn out to be lower, wider, and their maxima move backwards to small ω when collision frequency is considered through the Mermin response function. This fact is more noticeable in the high degeneracy limit. Of course, here again, classical approximation is closer to the exact case but the differences have diminished due to the collisions. At any rate we will consider the Mermin function with the exact degeneracy and collision frequency as the most appropriate dielectric response for calculating the ion stopping in the next section.

III. ELECTRONIC STOPPING

In the dielectric formalism, the formula for calculating the ion electronic stopping in any target is very well-known. The

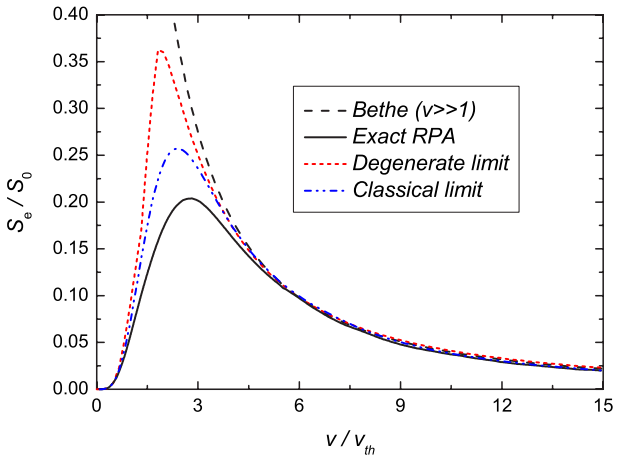

FIG. 3. (Color online) RPA proton electronic stopping as a function of proton velocity in a $T=10$ eV and $n_e=10^{23}$ cm^{-3} plasma ($D=0.785$). It is compared to the Bethe formula at high velocities and to degenerate and classical limits. Stopping forces are normalized to $S_0=(Zk_F)^2$.

electronic stopping for a swift pointlike ion with charge Z traveling with constant velocity $\mathbf{v}$ through a target plasma defined by its energy loss function is

$$S_e(v) = \frac{2Z^2}{\pi v^2}\int_0^\infty \frac{dk}{k}\int_0^{kv} d\omega\omega \,\mathrm{Im}\left[\frac{-1}{\epsilon(k,\omega)}\right] \text{(a.u.)}, \quad (18)$$

where $\mathrm{Im}\left[\frac{-1}{\epsilon(k,\omega)}\right]$ is any of the energy loss functions stated before. For proton velocities $v \gtrsim v_{th}$, where v_{th} is the thermal velocity of the target electrons, the perturbation parameter $\xi=Z/v$ is smaller than one, so the electronic stopping can be determined using the random phase approximation (RPA).

Figure 3 represents the proton electronic stopping as a function of the proton velocity in a $T=10$ eV and $n_e=10^{23}$ cm^{-3} plasma, not considering damping and normalized to $S_0=(Zk_F)^2$. The coupling parameter value is obtained from plasma temperature and electron density $\Gamma=0.184\lesssim 1$ which indicates that we are in the limit of weak coupling plasmas. The electron stopping is compared to the Bethe formula at high velocities. Regarding plasma degeneracy, $D=0.785$, the stopping graph is contrasted with the high degeneracy limit, Eqs. (8) and (13); and with the classical limit, Eqs. (9) and (14). Classical approximation is better than the high degeneracy one, but differs too much from the exact result. The maximum relative error is about 27% at $v=1.898v_{th}$ which is an important discrepancy to bear in mind in future energy deposition and proton range calculations.

Then we are going to see quite well the low and the high degeneracy limits approach the exact quantum mechanical result for plasmas of different degeneracy. Figure 4 displays the same graphs as in Fig. 3 but for different plasma temperatures and densities, i.e., for different values of the degeneracy parameter D. Case (a) corresponds to a $T=100$ eV and $n_e=10^{23}$ cm^{-3} plasma with $D=0.079$. Case (b) corresponds to a $T=1$ eV and $n_e=10^{23}$ cm^{-3} plasma with $D=7.854$. Case (c) corresponds to $T=10$ eV and $n_e=10^{22}$ cm^{-3} plasma with $D=0.169$; and finally case (d) corresponds to $T=10$ eV and $n_e=10^{24}$ cm^{-3} plasma with $D=3.645$.

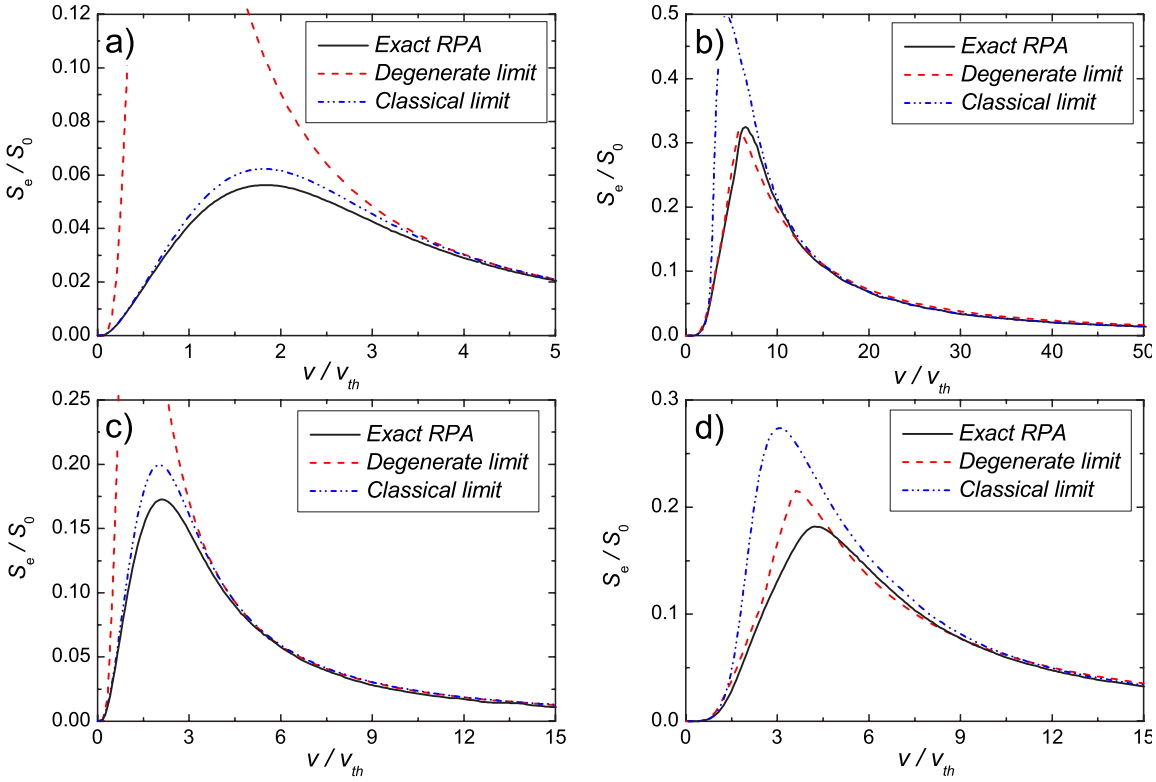

FIG. 4. (Color online) The same as in Fig. 3 but for different kinds of plasma targets: (a) $T=100$ eV and $n_e=10^{23}$ cm^{-3} ($D=0.079$), (b) $T=1$ eV and $n_e=10^{23}$ cm^{-3} ($D=7.854$), (c) $T=10$ eV and $n_e=10^{22}$ cm^{-3} ($D=0.169$), and (d) $T=10$ eV and $n_e=10^{24}$ cm^{-3} ($D=3.645$).

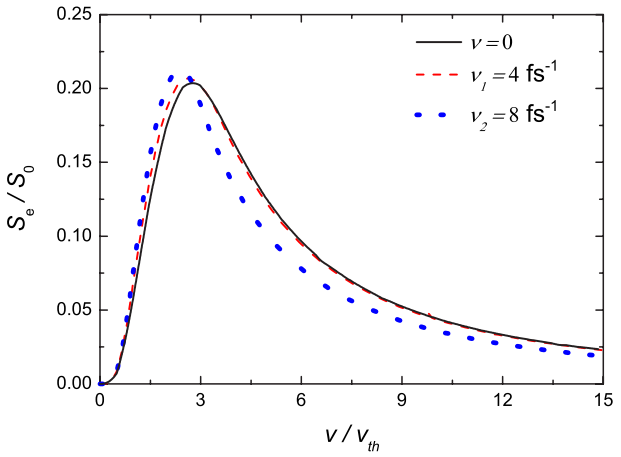

FIG. 5. (Color online) Proton electronic stopping as a function of its velocity in a $T=10$ eV and $n_e=10^{23}$ cm^{-3} plasma ($\Gamma=0.184$) for different values of the electron-electron collision frequency. Stopping forces are normalized to $S_0=(Zk_F)^2$.

The high degeneracy limit is the same for all plasma cases with the same electron density as this approximation does not depend on temperature. As an example we can analyze proton electronic stopping in three plasmas with the same electron density $n_e=10^{23}$ cm^{-3}, Figs. 3, 4(a), and 4(b). We see that by diminishing temperature, i.e., by increasing the degeneracy parameter, the exact stopping approaches to the high energy limit, but differences are still significant. For a plasma with the highest degeneracy parameter, $D=7.854$, the relative error is around 10%. On the other hand, by increasing temperature the degeneracy parameter decreases and the exact stopping approaches to the classical limit. For a sufficient low value of it, $D=0.079$, the classical approximation still differs from the exact value, 10% at $v=1.695v_{th}$. These last facts could indicate, for example, that we will make a significant error of the temperature increase of an ICF target due to protons ignition if we calculate their energy loss from any of the common latter approximations.

Next we will study how proton electronic stopping varies with electron density of plasmas with the same temperature $T=10$ eV. Figure 4(c) corresponds to an electron density of $n_e=10^{22}$ cm^{-3}, Fig. 3 corresponds to $n_e=10^{23}$ cm^{-3}, and Fig. 4(d) to $n_e=10^{24}$ cm^{-3}. As electron density increases, the degeneracy parameter also increases. For the lowest value analyzed $n_e=10^{22}$ cm^{-3}, corresponding to $D=0.169$, the exact calculation looks like the classical result while the highest $n_e=10^{24}$ cm^{-3}, with $D=3.645$, looks like the high degeneracy limit. In the intermediate case, $n_e=10^{23}$ cm^{-3} and with $D=0.785$, approximates better to the classical result. However, again, there are substantial differences with the exact calculation in the three examples.

Once we have seen the errors we make when we use high degeneracy or classical limits to calculate electronic stopping, we are going to study the error due to the fact of including or not including target electron-electron collisions in this calculation. We introduce the collision frequency ν as a free parameter in Eq. (18) through Mermin dielectric function, Eq. (16). Figure 5 shows proton stopping as a function of its velocity in a plasma with electron density $n_e=10^{23}$ cm^{-3} and temperature $T=10$ eV. These graphs are obtained by using the quantum mechanical dielectric function considering the exact degeneracy, $D=0.785$, since, as we have seen above, the classical and high degeneracy approximations induce to a relative error. The solid line corresponds to the frequency value $\nu=0$, that is to say, not considering collisions as in Fig. 3. The dashed line is the result for $\nu_1=4$ fs^{-1} and the dotted line for $\nu_2=8$ fs^{-1}. These parameter values are close to the value obtained from Eq. (17). It is observed that the electronic stopping curves narrow, their maximum values increase, and they are situated at lower velocities when ν increases. When the curves narrow, the result for velocities lower than the velocity at maximum enhances while for higher velocities drops significantly. Differences between not considering collisions and considering them, in the case of $\nu_1=4$ fs^{-1}, are about 6% for lower velocities than the velocity at the maximum.

In the next figure, we observe the effects of electron-electron collisions on the electronic stopping for plasmas of different degeneracy. We also study how the stopping evolves with increasing collision frequency. Figure 6 displays the same calculations as in Fig. 5 but for different plasma targets and for different values of the electron-electron collision frequency ν. Case 6(a) corresponds to a $T=100$ eV and $n_e=10^{23}$ cm^{-3} plasma with $\Gamma=0.031$. Case 6(b) corresponds to a $T=1$ eV and $n_e=10^{23}$ cm^{-3} plasma with $\Gamma=0.372$. Case 6(c) corresponds to $T=10$ eV and $n_e=10^{22}$ cm^{-3} plasma with $\Gamma=0.131$; and finally case 6(d) corresponds to $T=10$ eV and $n_e=10^{24}$ cm^{-3} plasma with $\Gamma=0.153$. For all four cases the maximum occurs at smaller or similar velocities than for the calculations without including collisions. New values considering collisions enhance for velocities smaller than the velocity at maximum and smoothly decreases for higher velocities. These effects for plasmas with the same density, $n_e=10^{23}$ cm^{-3}, case 6(a), Fig. 5, and case 6(b), are more pronounced as the target plasma is colder. These effects for plasmas with the same temperature, $T=10$ eV, case 6(c), Fig. 5, and case 6(d), are less significant increasing plasma density. It looks like that these effects are more remarkable as target plasma is more degenerate and coupled but not when we increase plasma density, because at the same time we are increasing the main characteristic frequency of the plasma, the plasma frequency, ω_p. When we continue increasing the collision frequency latter effects are magnified except for the most dense plasma case, 6(d), where these effects are not notable. It seems that when we increase collision frequency the first effect is enhancing the stopping maximum narrowing the graph at the same time. If we continue increasing the collision frequency the stopping maximum finally decreases expanding the graph again. For the $\nu_1=4$ fs^{-1} value, deviations are around 20% compared with the not damping result in the case of the least dense plasma analyzed, case 6(c).

IV. CONCLUSIONS

In this work, the effects of target electron-electron collisions in the electronic stopping of protons in plasmas of any degeneracy has been examined. The electronic stopping is

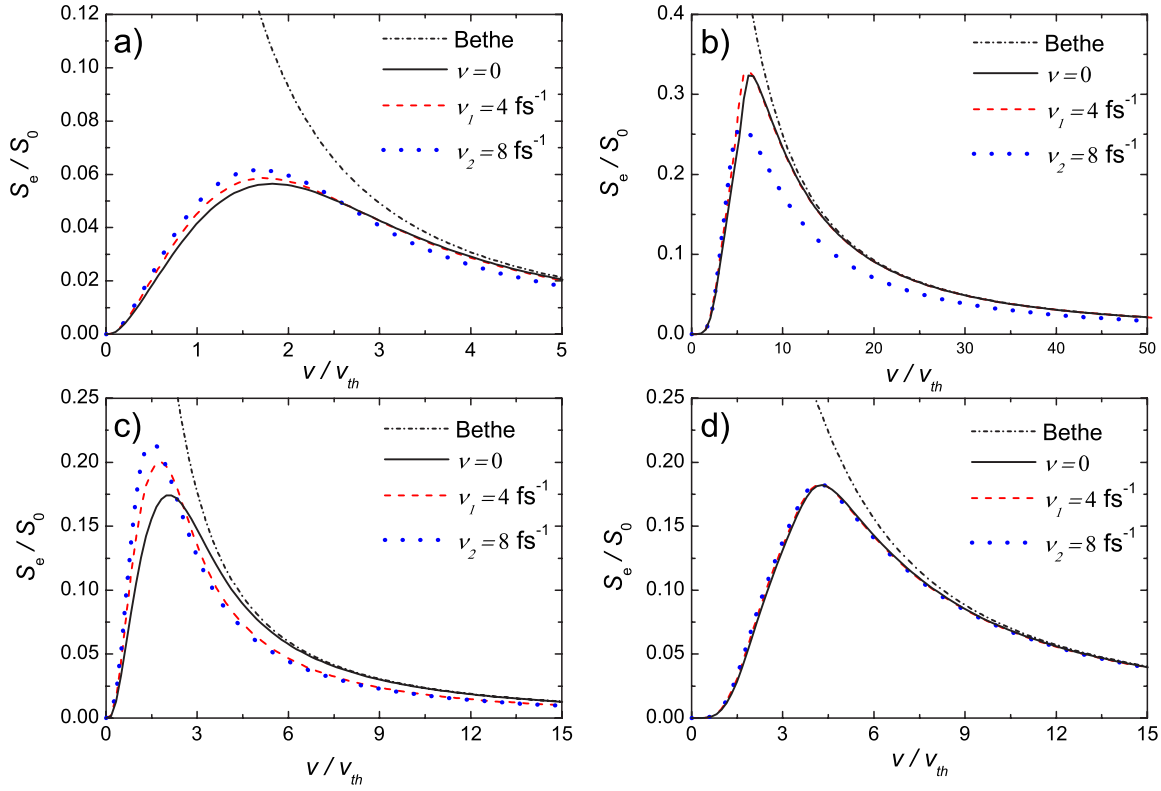

FIG. 6. (Color online) The same as in Fig. 5 but for different kinds of plasma targets: (a) $T=100$ eV and $n_e=10^{23}$ cm^{-3} ($\Gamma=0.031$), (b) $T=1$ eV and $n_e=10^{23}$ cm^{-3} ($\Gamma=0.372$), (c) $T=10$ eV and $n_e=10^{22}$ cm^{-3} ($\Gamma=0.131$), and (d) $T=10$ eV and $n_e=10^{24}$ cm^{-3} ($\Gamma=0.153$).

due to the free electrons as plasma targets are considered fully ionized. Their electronic density is around solid values $n_e \simeq 10^{23}$ cm^{-3} and their temperature around $T \simeq 10$ eV, which are very interesting for ICF.

To calculate the electronic stopping, we have used the exact quantum mechanical analysis which takes into account the degeneracy of the target plasma. It has been checked that if we employ classical or degenerate approximations instead, we obtain a considerable error. This error could be around 30% in some cases which can produce bigger mistakes in later energy deposition and projectile range studies.

Moreover, we have considered electron-electron collisions in the exact quantum mechanical calculation. For all plasma cases the maximum appears at smaller velocities than for the calculations without considering collisions. The stopping remains equal or enhances for velocities smaller than or equal to the velocity at maximum while decreases a great deal for higher velocities. Increasing collision frequency parameter magnifies later effects. Differences with the same results but not taking into account these collisions are about 20%.

The main conclusion of this work is that proton electronic stopping in these kinds of target plasmas cannot be calculated realistically without using the exact quantum mechanical analysis that considers the degeneracy of the plasma, and without contemplating electron-electron collisions.

ACKNOWLEDGMENTS

This work was financed by the Spanish Ministerio de Educación y Ciencia (under Project No. FIS2006-05389) and the Consejería de Educación y Ciencia de la Junta de Comunidades de Castilla-La Mancha (under Project No. PAI-05-071).

[1] C. Deutsch, Laser Part. Beams **2**, 449 (1984).
[2] M. Roth *et al.*, Phys. Rev. Lett. **86**, 436 (2001).
[3] E. Fermi, Phys. Rev. **57**, 485 (1940).
[4] J. Lindhard, K. Dan. Vidensk. Selsk. Mat. Fys. Medd. **28**(8), 1 (1954).
[5] J. Lindhard and A. Winther, K. Dan. Vidensk. Selsk. Mat. Fys. Medd. **34**(4), 1 (1964).
[6] D. Pines and D. Bohm, Phys. Rev. **85**, 338 (1952).
[7] A. I. Akhiezer and A. G. Sitenko, Zh. Eksp. Teor. Fiz. **23**, 161 (1952).
[8] G. Zwicknagel, C. Toepffer, and P. G. Reinhard, Phys. Rep. **309**, 117 (1999).
[9] R. C. Arnold and Y. Meyer-ter-Vehn, Rep. Prog. Phys. **50**, 559 (1987).
[10] N. D. Mermin, Phys. Rev. B **1**, 2362 (1970).
[11] A. K. Das, J. Phys. F: Met. Phys. **5**, 2035 (1975).

[12] A. Selchow, G. Ropke, and K. Morawetz, Nucl. Instrum. Methods Phys. Res. A **441**, 40 (2000).
[13] K. Morawetz and U. Fuhrmann, Phys. Rev. E **61**, 2272 (2000); **62**, 4382 (2000).
[14] G. S. Atwal and N. W. Ashcroft, Phys. Rev. B **65**, 115109 (2002).
[15] J. C. Ashley and P. M. Echenique, Phys. Rev. B **35**, 8701 (1987).
[16] I. Abril, R. Garcia-Molina, C. D. Denton, F. J. Perez-Perez, and N. R. Arista, Phys. Rev. A **58**, 357 (1998).
[17] C. D. Denton, I. Abril, M. D. Barriga-Carrasco, R. Garcia-Molina, G. H. Lantschner, J. C. Eckardt, and N. R. Arista, Nucl. Instrum. Methods Phys. Res. B **193**, 198 (2002).
[18] M. Lampe, Phys. Rev. **170**, 306 (1968).
[19] E. Flowers and N. Itoh, Astrophys. J. **206**, 218 (1976).
[20] V. A. Urpin and D. G. Yakovlev, Sov. Astron. **24**, 126 (1980).
[21] J. C. Ashley, Nucl. Instrum. Methods **170**, 197 (1980).
[22] J. C. Ashley and P. M. Echenique, Phys. Rev. B **31**, 4655 (1985).
[23] H. B. Nersisyan, A. K. Das, and H. H. Matevosyan, Phys. Rev. E **66**, 046415 (2002).
[24] E. L. Clark *et al.*, Phys. Rev. Lett. **84**, 670 (2000).
[25] R. A. Snavely *et al.*, Phys. Rev. Lett. **85**, 2945 (2000).
[26] M. Roth *et al.*, Phys. Rev. ST Accel. Beams **5**, 061301 (2002).
[27] M. Hegelich *et al.*, Phys. Rev. Lett. **89**, 085002 (2002).
[28] J. Fuchs *et al.*, Nat. Phys. **2**, 48 (2006).
[29] B. M. Hegelish *et al.*, Nature (London) **439**, 441 (2006).
[30] H. Schwoerer *et al.*, Nature (London) **439**, 445 (2006).
[31] R. Garcia-Molina and M. D. Barriga-Carrasco, Phys. Rev. A **68**, 054901 (2003).
[32] M. D. Barriga-Carrasco and R. Garcia-Molina, Phys. Rev. A **68**, 062902 (2003).
[33] M. D. Barriga-Carrasco and R. Garcia-Molina, Phys. Rev. A **70**, 032901 (2004).
[34] M. D. Barriga-Carrasco and G. Maynard, Laser Part. Beams **24**, 55 (2006).
[35] M. D. Barriga-Carrasco, Phys. Rev. E **73**, 026401 (2006).
[36] S. Skupsky, Phys. Rev. A **16**, 727 (1977).
[37] N. R. Arista and W. Brandt, Phys. Rev. A **23**, 1898 (1981).
[38] G. Maynard and C. Deutsch, Phys. Rev. A **26**, 665 (1982).
[39] M. D. Barriga-Carrasco and G. Maynard, Laser Part. Beams **23**, 211 (2005).
[40] N. R. Arista and W. Brandt, Phys. Rev. A **29**, 1471 (1984).
[41] B. D. Fried and S. D. Conte, *The Plasma Dispersion Function* (Academic, New York, 1961).
[42] T. Peter and J. Meyer-ter-Vehn, Phys. Rev. A **43**, 1998 (1991).
[43] S. I. Braginskii, Zh. Eksp. Teor. Fiz. **33**, 459 (1957) (in Russian).
[44] L. Spitzer, *Physics of Fully Ionized Gases* (Interscience, New York, 1961).